Supporting information for: Dynamics in the active site of β-secretase: A network analysis of atomistic simulations

Sabyashachi Mishra,* and Amedeo Caflisch*

Department of Biochemistry, University of Zurich, Zurich, Switzerland

E-mail: s.mishra@bioc.uzh.ch; caflisch@bioc.uzh.ch

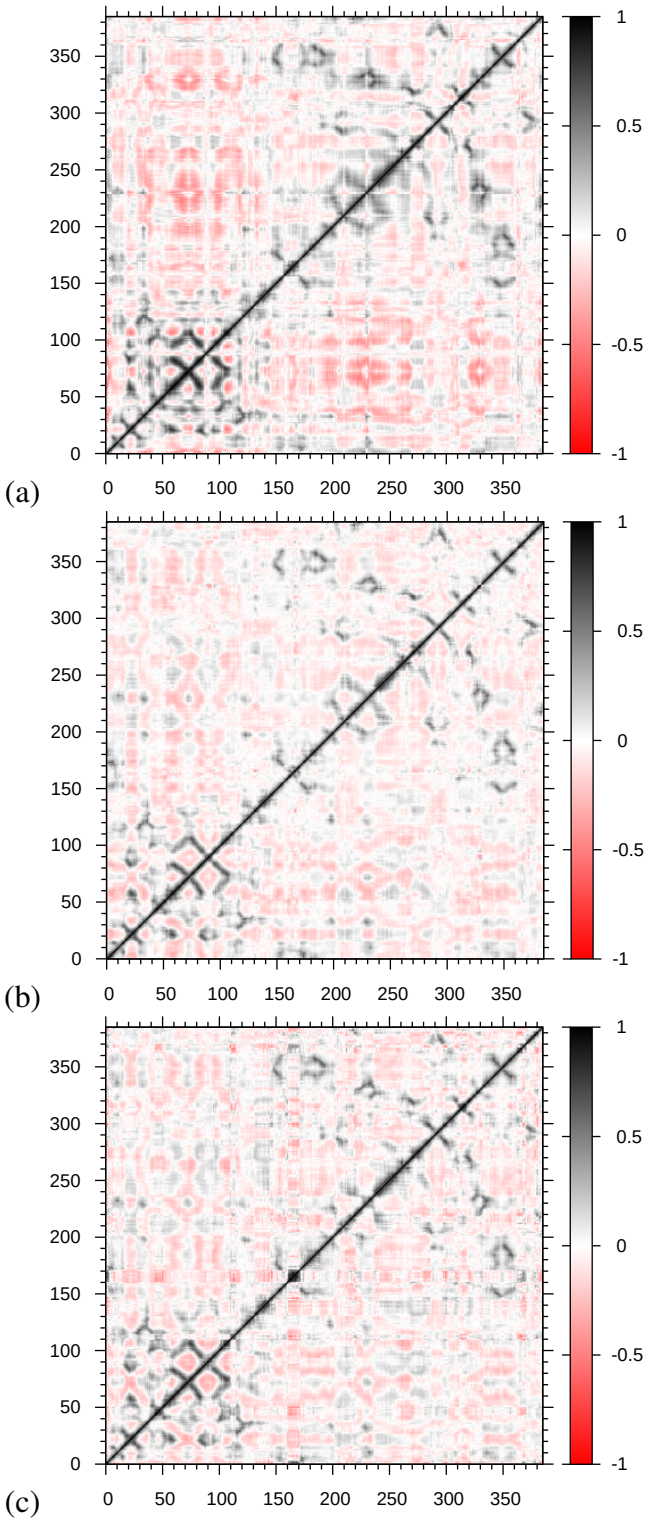

Figure S1: BACE C_α dynamic cross correlation map obtained by averaging over all the conformations in the last 30 ns of a randomly picked MD trajectory of BACE-substrate simulation when substrate is in (a) reactant, (b) intermediate, and (c) product form. The highly correlated region between BACE residues 1 to 120 arises due to the presence of several β-sheets in that region. The similar C_α cross correlation maps show that the correlated motion in BACE are similar in all three states of the substrate. Similar results are obtained from other trajectories.

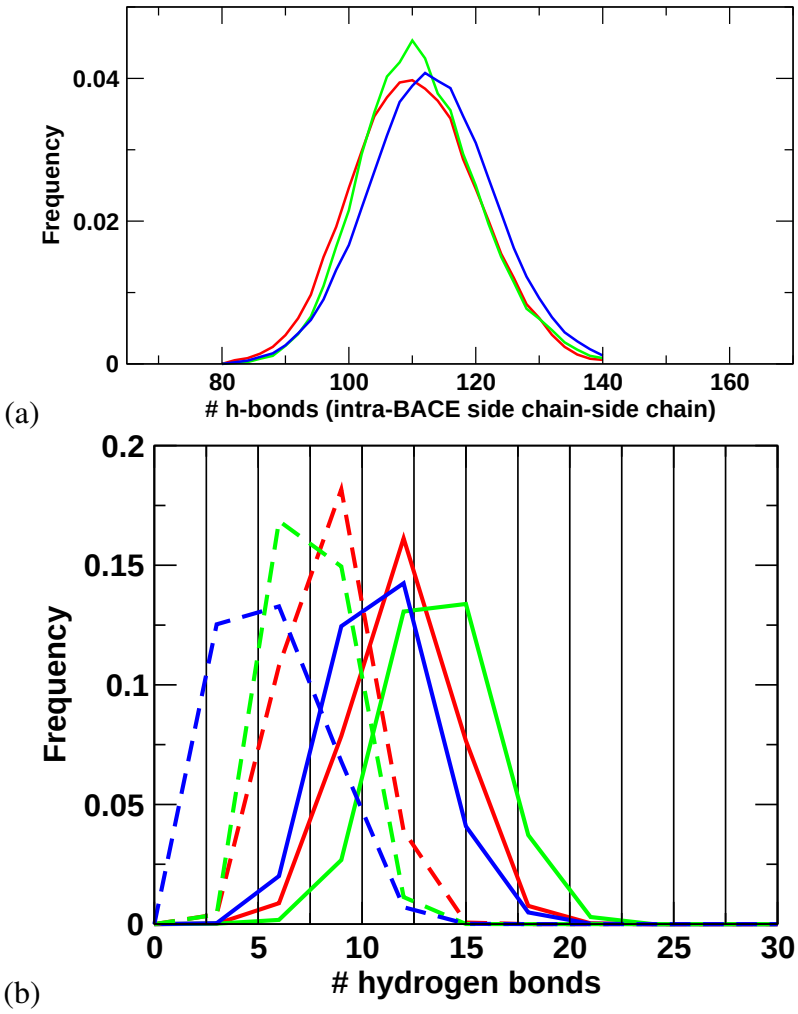

Figure S2: Distribution of number of hydrogen bonds (a) within BACE (side chain-side chain) (b) between four N-terminal residues of the substrate and all atoms in the system (solid lines), and between C-terminal residues of the substrate and all atoms in the system (dashed lines). The substrate in reactant, intermediate, and product form are shown by red, green, and blue lines, respectively.

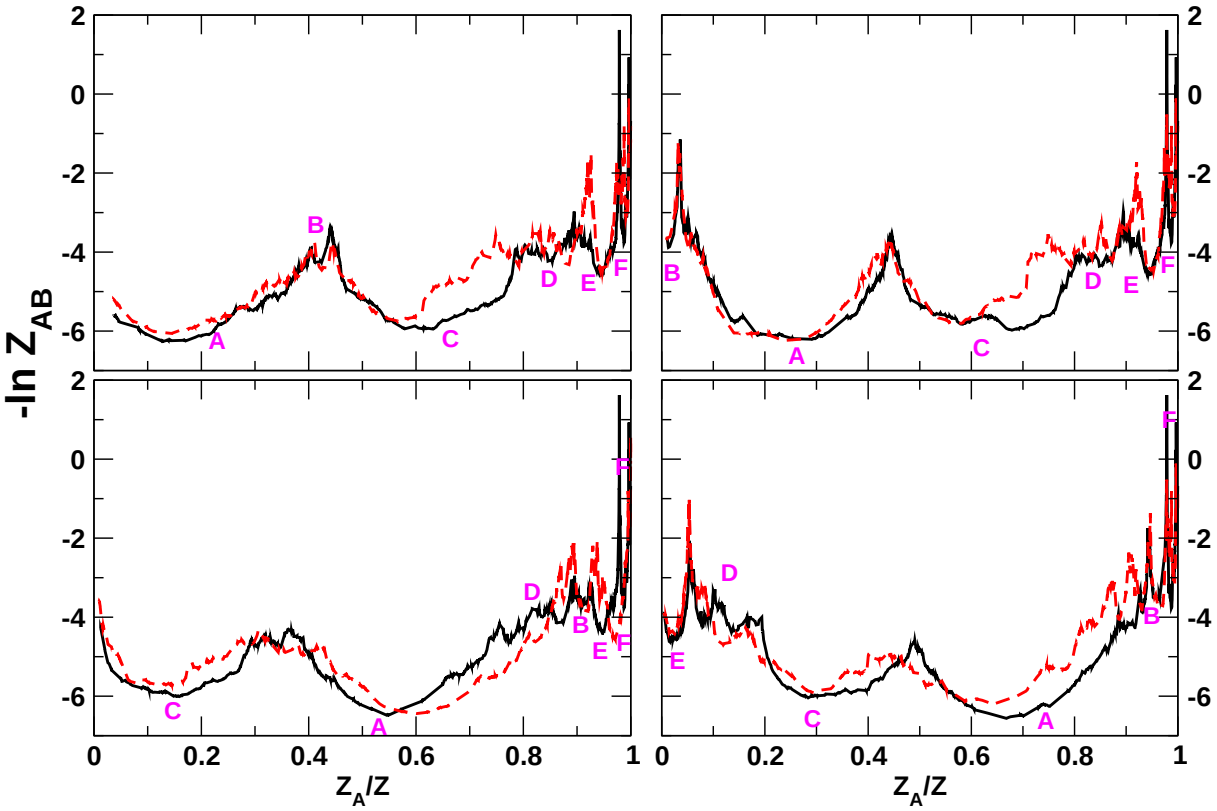

Figure S3: Diffusivity tests. The cFEPs from the most populated node of different basins (black line) for BACE-reactant simulations. The red curve shows the cFEP when every second snapshot of MD trajectory is considered for clustering and cFEP calculation. The resulting cFEP is shifted downward along the y axis by $\ln\sqrt{2}$ (Ref 34 in the main text), for visual inspection of the diffusivity test. In the first basin on the left of each profile, the overlapping black and red curves confirm the diffusive nature of dynamics and thereby validate the clustering procedure. Note that the deviations after the first barrier on the left are expected due to different order of nodes along Z_A/Z for dt and 2dt saving intervals.

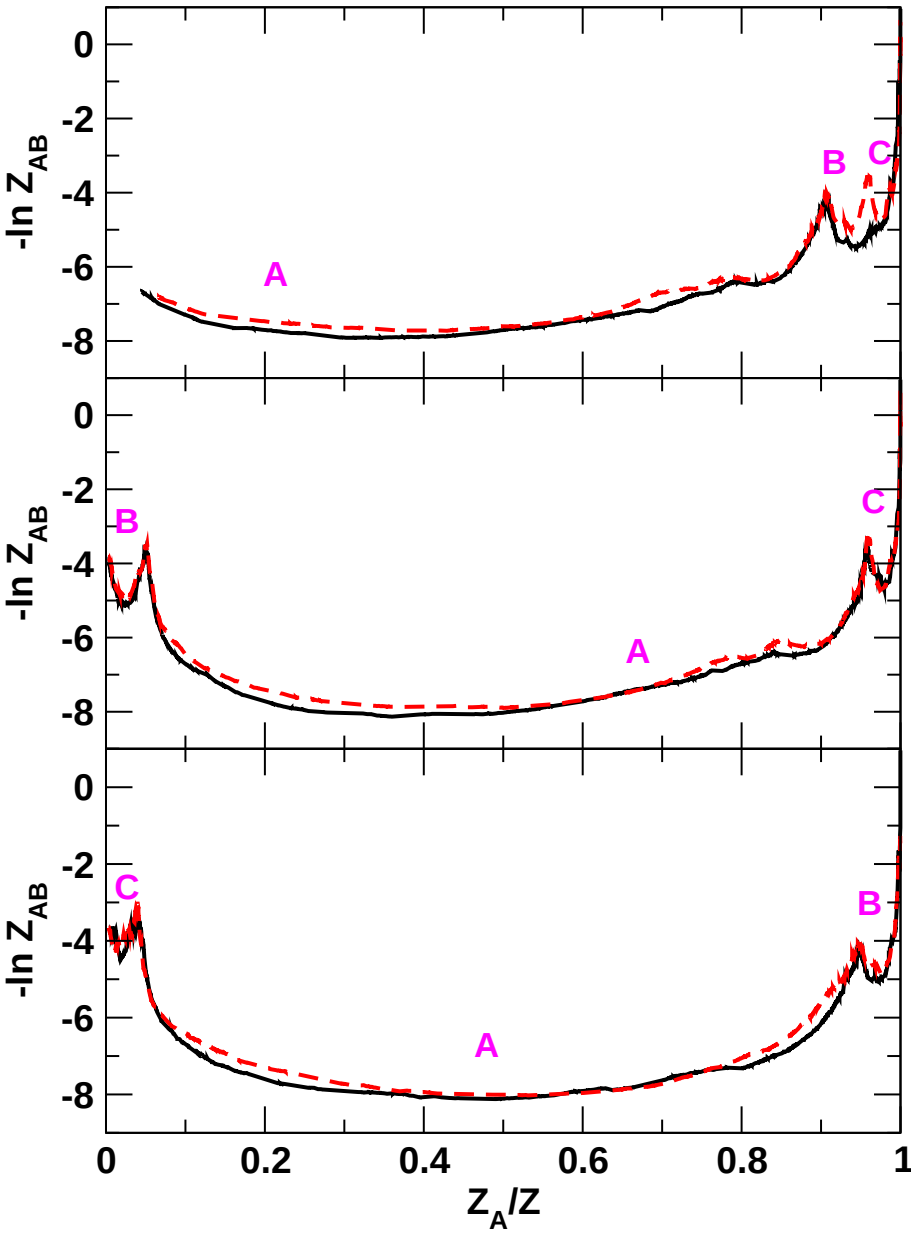

Figure S4: Same as in Figure S3 for BACE-intermediate simulations.

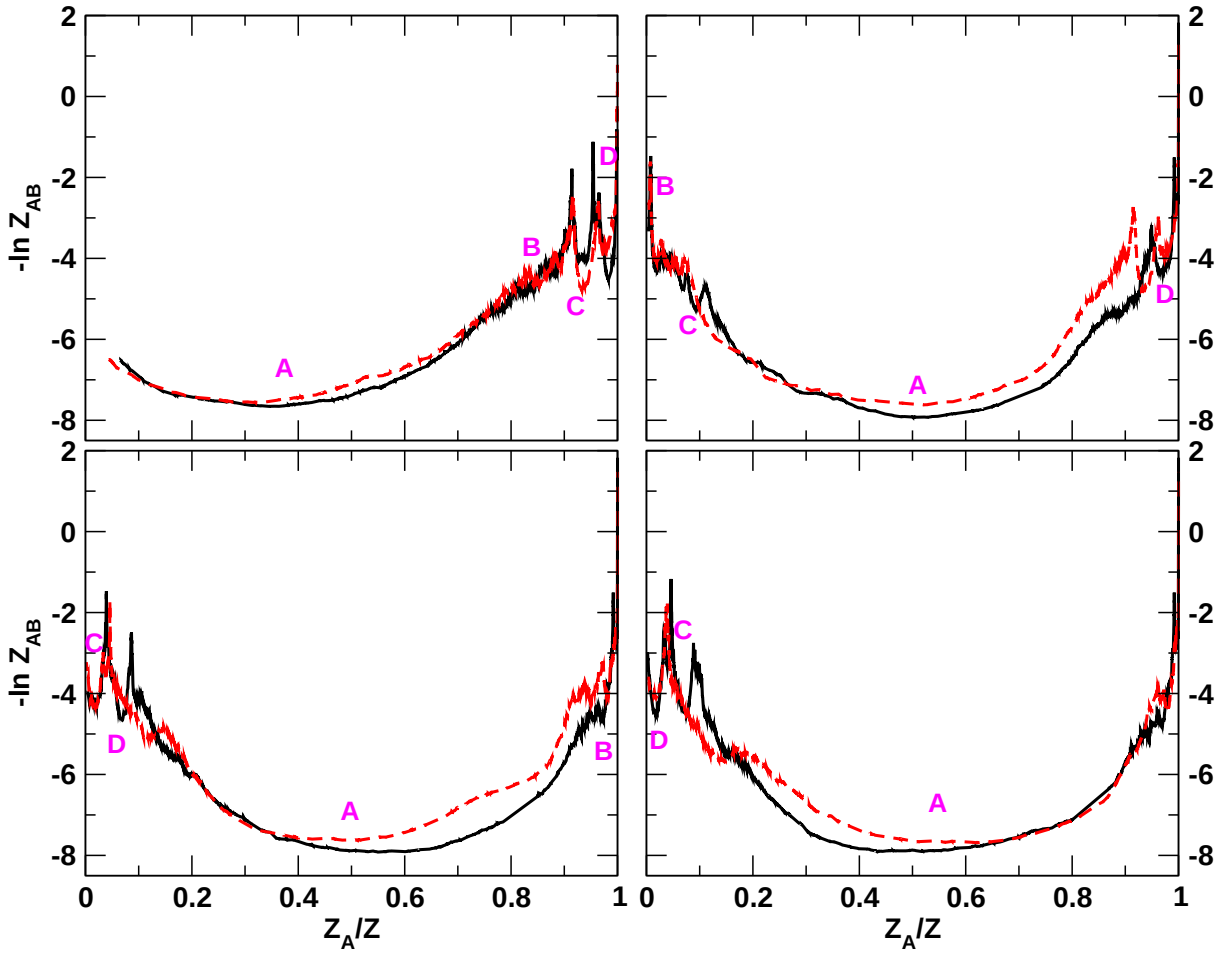

Figure S5: Same as in Figure S3 for BACE-product simulations.

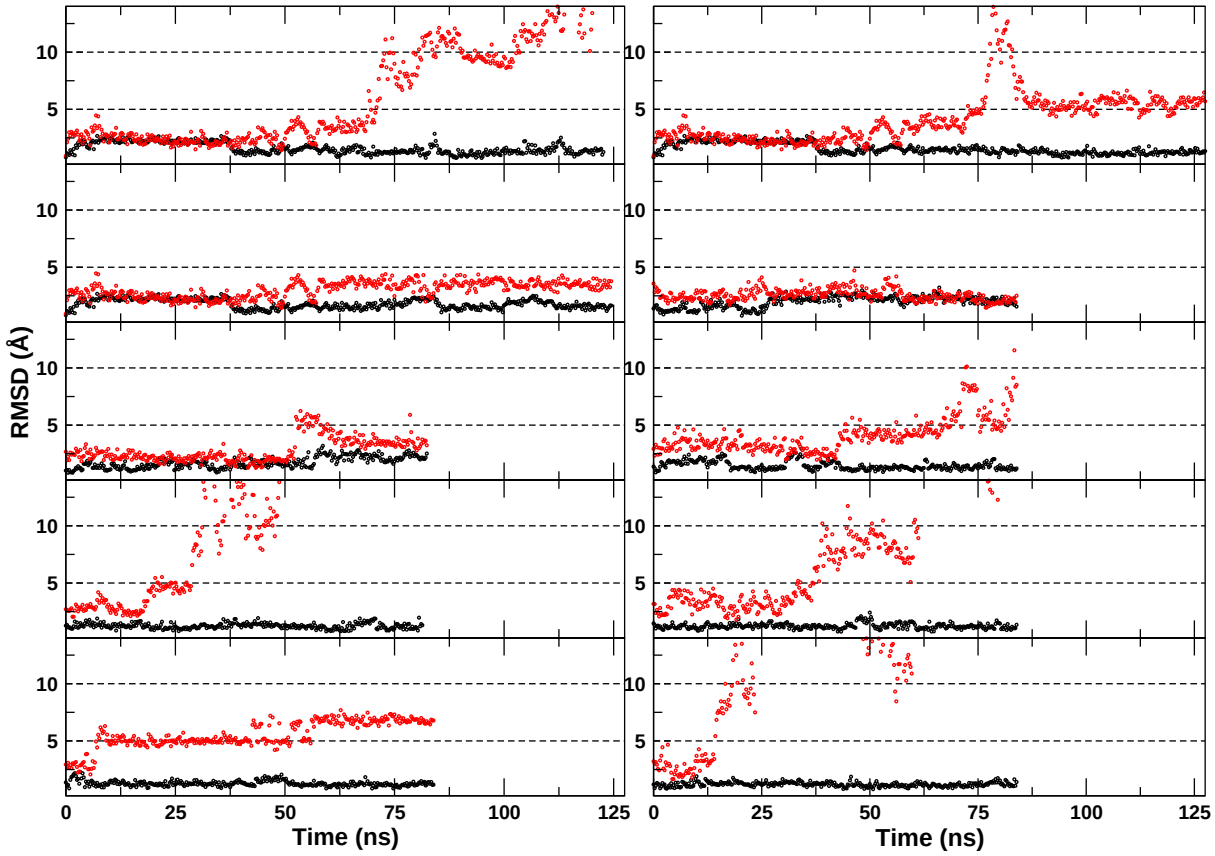

Figure S6: Time evolution of C_α RMSD of the C-terminus of the cleaved product (red) and heavy atom RMSD of the flap, i.e., residue 67 to 77 (black) for 10 MD trajectories. A structural fitting of BACE C_α atoms was done prior to the RMSD calculations with respect to the X-ray structure (PDB ID 1FKN). The almost constant value of the flap RMSD indicates that the release of the C-terminal fragment of the product does not require opening of the flap.

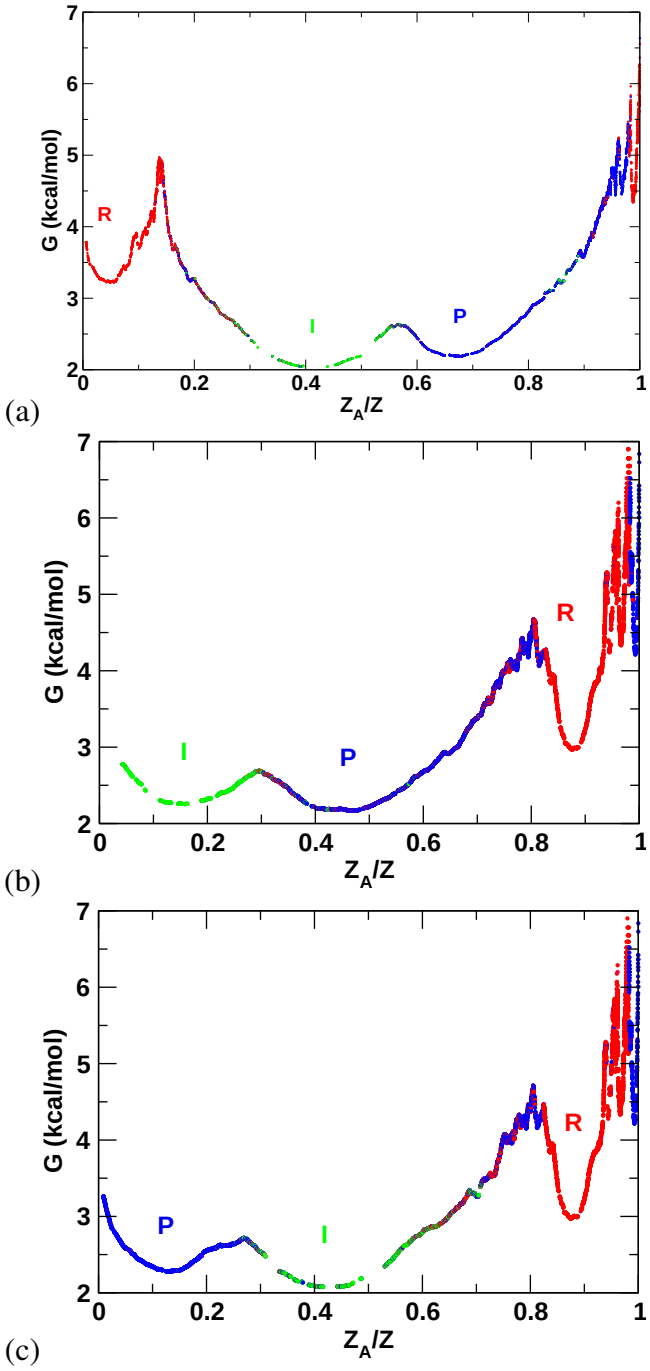

Figure S7: The cFEP starting from the most populated node of reactant (a), intermediate (b), and product (c) obtained from the DRMS clustering of all BACE-substrate snapshots. Each node is colored according to the fraction of its snapshots belonging to the reactant (red), intermediate (green), and product (blue) states. Figure (a) is identical to the Figure 9b of the main text, shown here for completeness.

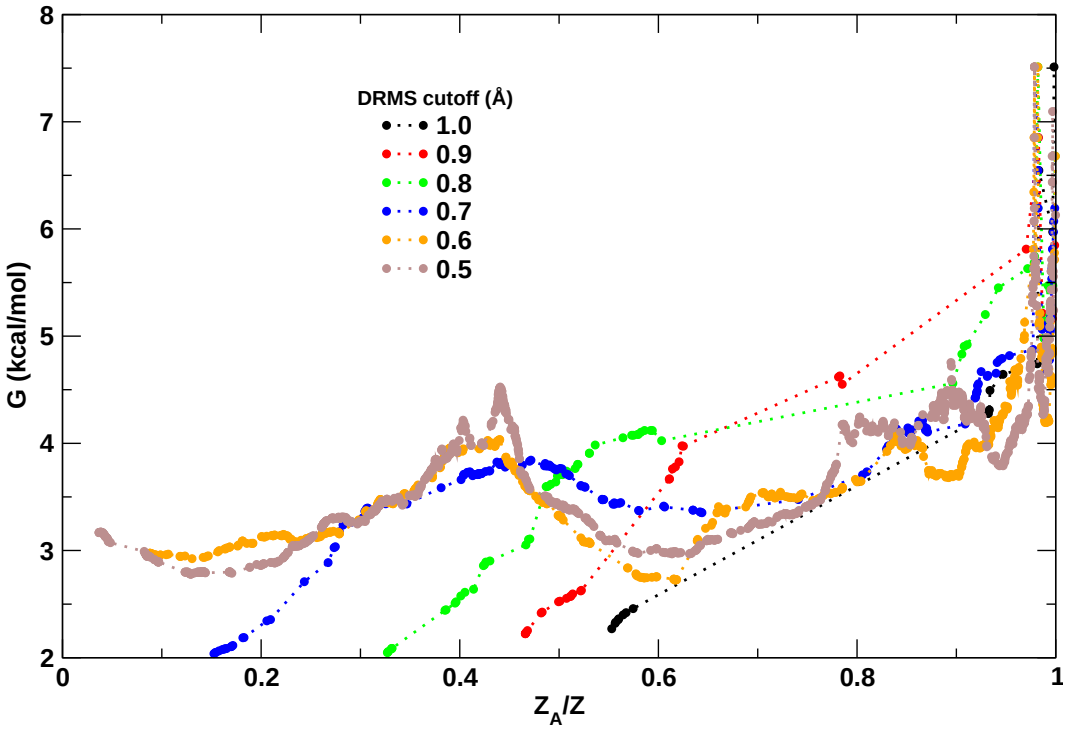

Figure S8: The cFEPs calculated from the most populated node of the networks obtained with different DRMS cutoff values. The free energy profiles with DRMS cutoff of 0.6 (orange) and 0.5 Å (brown) are similar. Hence the cFEP with DRMS cutoff of 0.5 Å (the converged cFEP) is used for subsequent basin analysis. Similar tests were also done for cFEP calculation of BACE-intermediate and BACE-product complexes (data not shown).

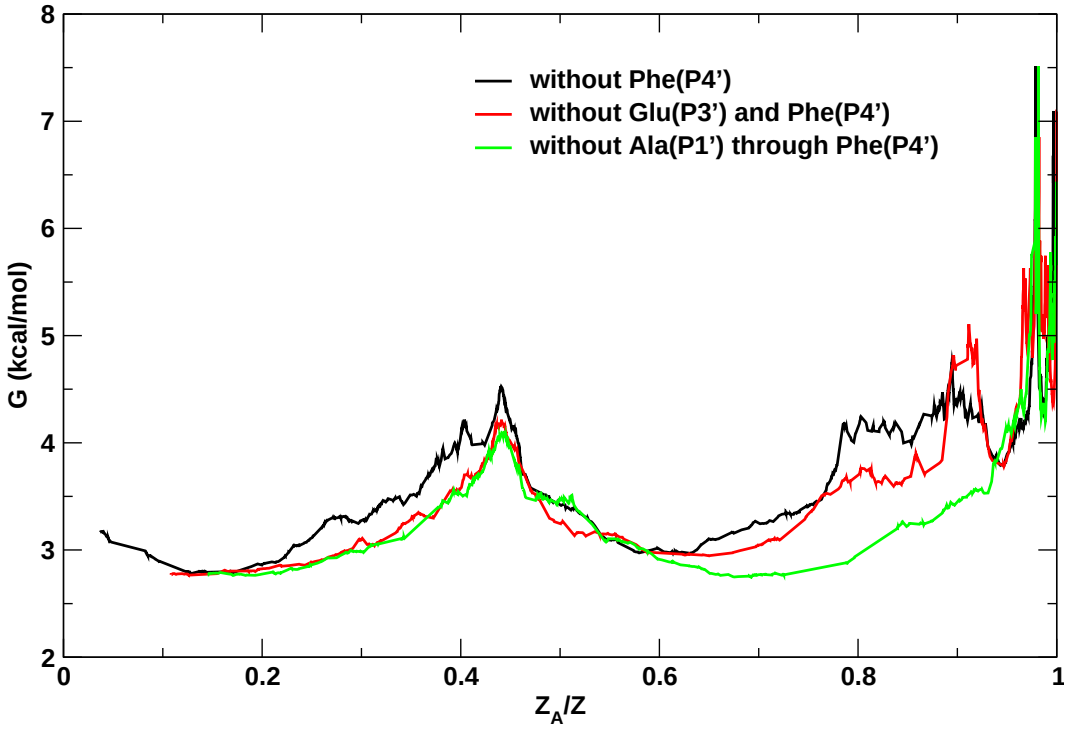

Figure S9: The cFEPs calculated from the most populated node of the networks obtained with different atom selections for the substrate in reactant form. The overall shape of cFEP is little affected with the changing atom selection suggesting the robustness of clustering. Note that, in these clustering and cFEP calculations only the (mentioned) substrate residues are ignored. Those BACE active site atoms involved in interactions with the ignored substrate residues are still there in the clustering procedure. Similar results are obtained for BACE-intermediate and BACE-product complexes (data not shown).

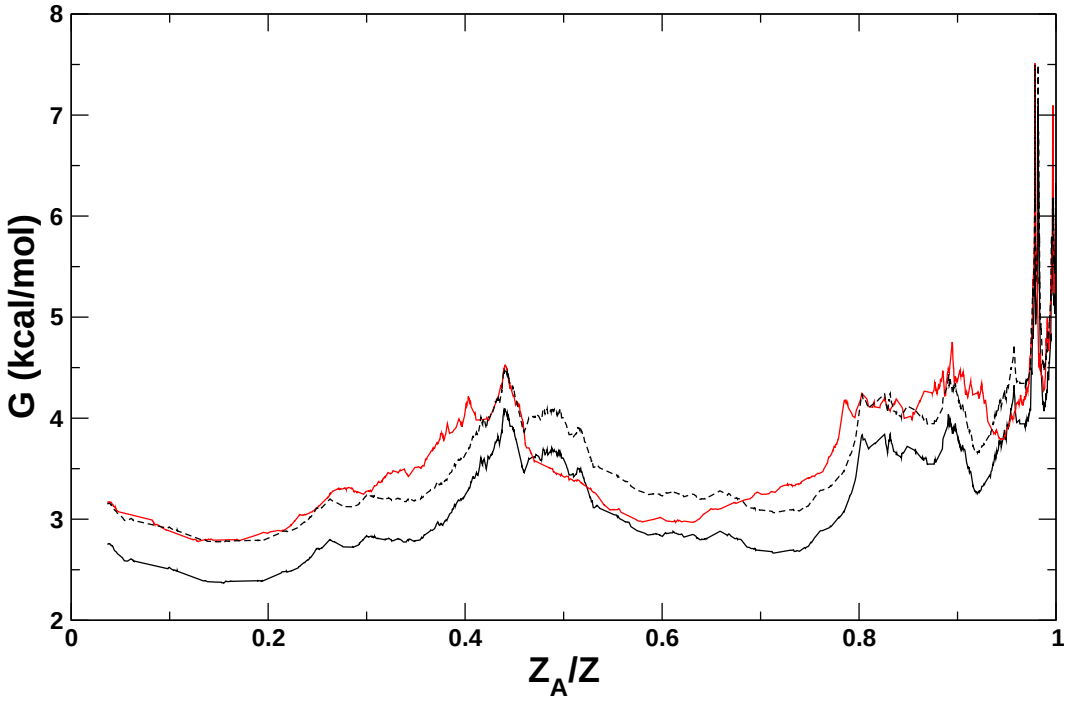

Figure S10: The cFEPs from the most populated node obtained from DRMS clustering of BACE-reactant trajectories without and with detailed balance (solid lines in red and black, respectively). Detailed balance is achieved by imposing symmetry in the transition matrix, i.e., $c_{ij} = c_{ji} = 0.5(c_{ij} + c_{ji})$, where c_{ij} is the number of transitions from node i to j observed in MD simulation. The dashed line is obtained when the cFEP with detailed balance is shifted by 0.4 kcal/mol along y-axis. The overall shape of the cFEP (until the first barrier) is not affected by imposing detailed balance. Similar results are obtained for BACE-intermediate and BACE-product complexes (data not shown).

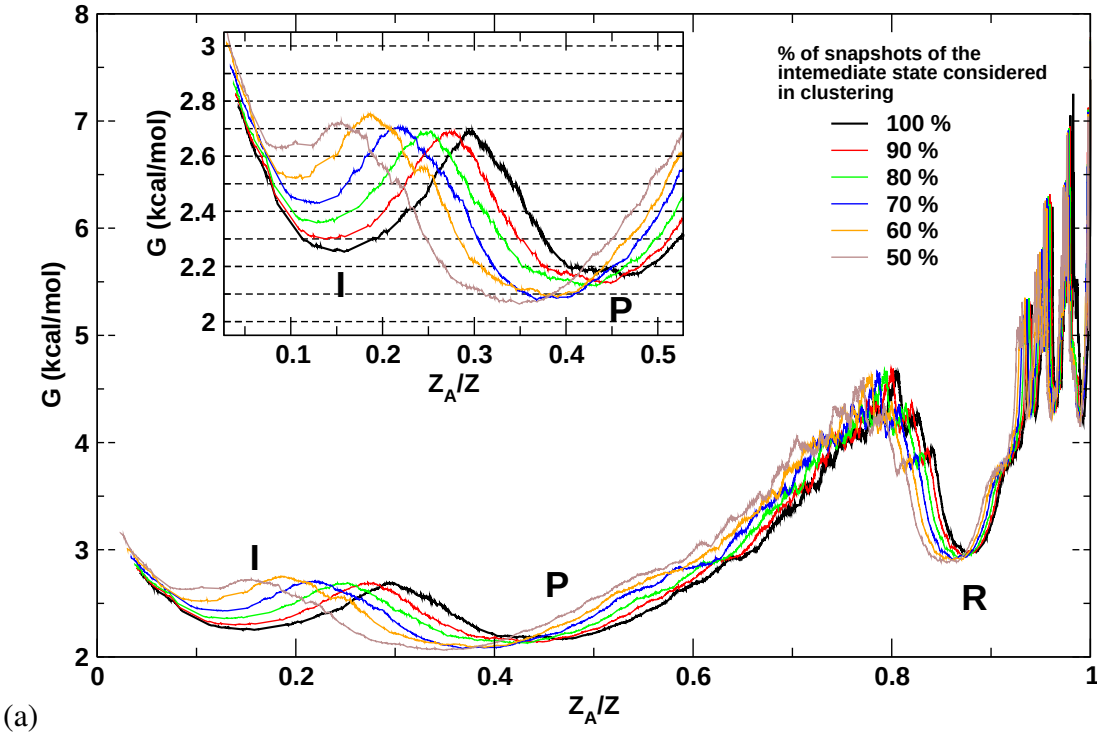

(a)

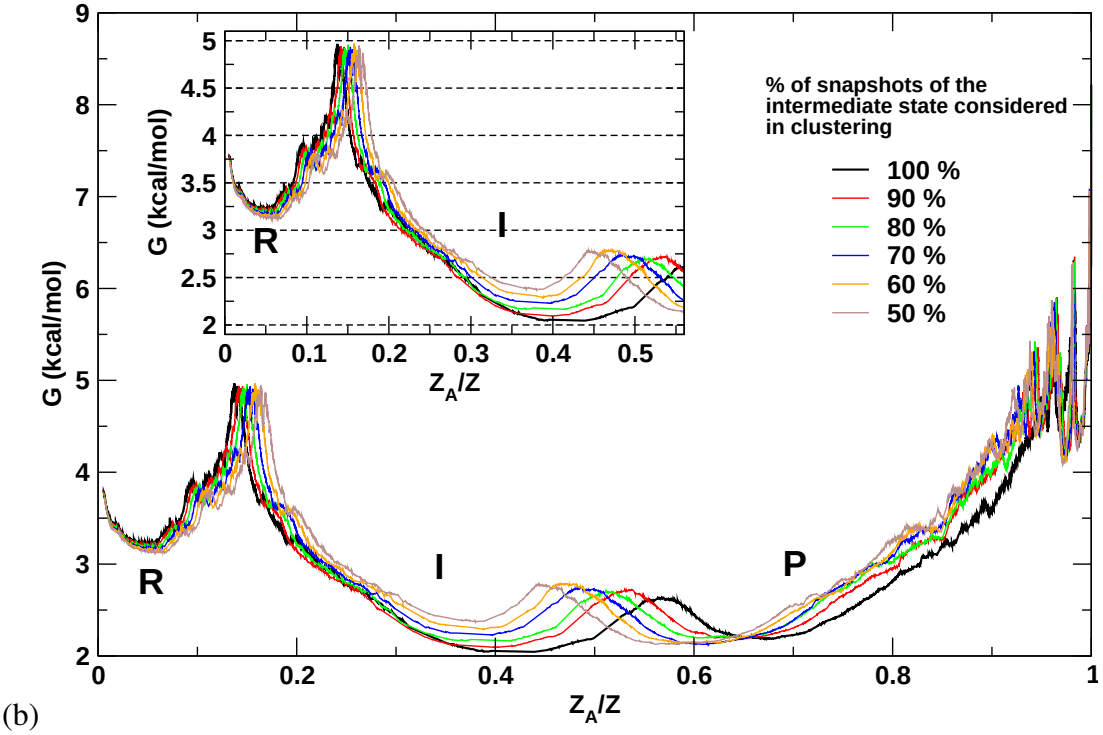

(b)

Figure S11: (a) The cFEPs from the most populated node (belongs to the intermediate state) when 50 to 100% of the snapshots from the intermediate state are considered in the DRMS clustering together with all snapshots of reactant and product states. The inset magnifies the first cFEP barriers. (b) Same as in (a), but the cFEPs are from the most populated node of the reactant state.

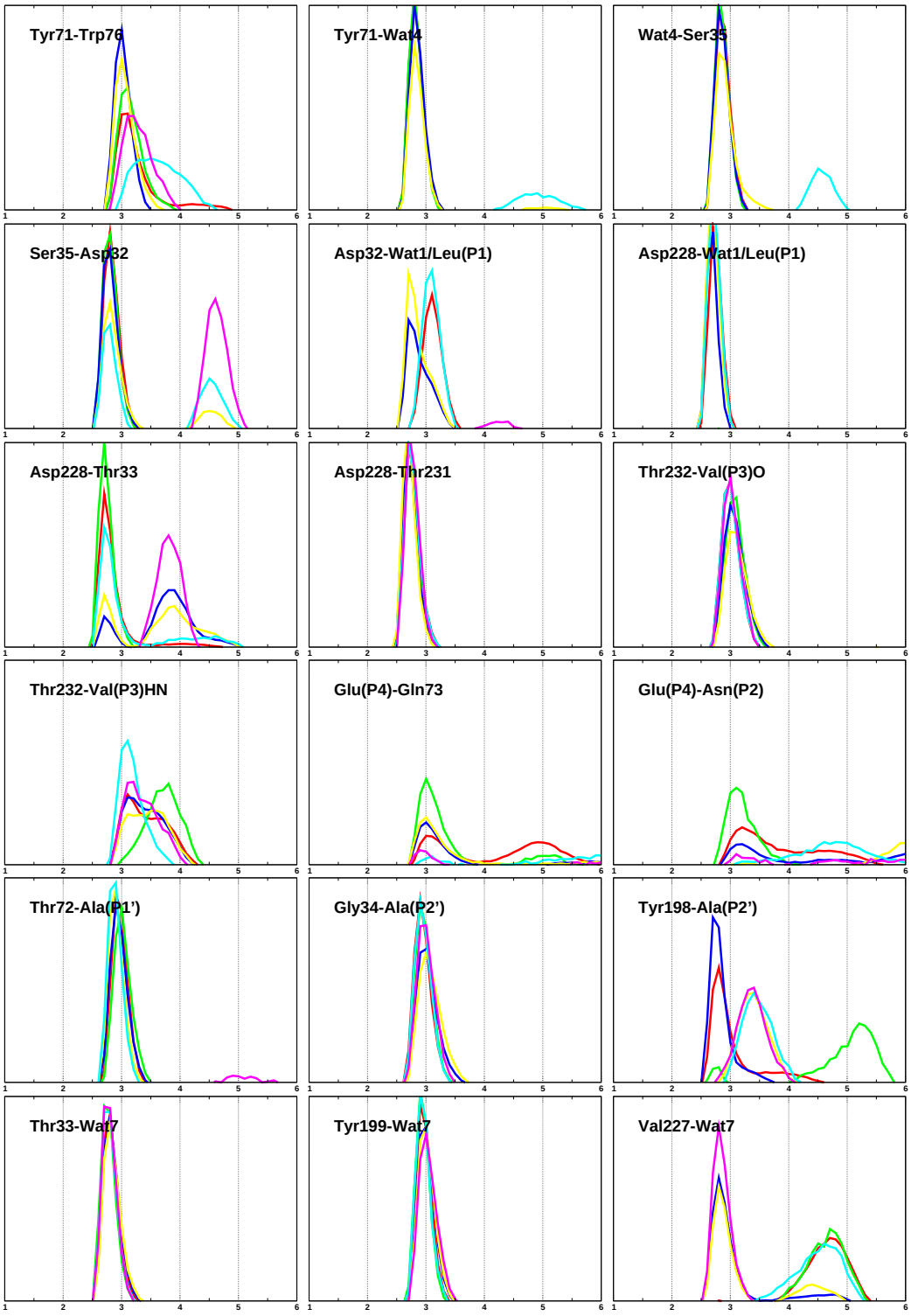

Figure S12: Distribution of the heavy-atom distances (in Å) of hydrogen bond partners in BACE active site and substrate (in reactant state) within each of the six cFEP basins (A through F) shown in Figure 4a of the main text. The distribution in the cFEP basins A through F are shown in red, green, blue, yellow, cyan, and magenta, respectively.

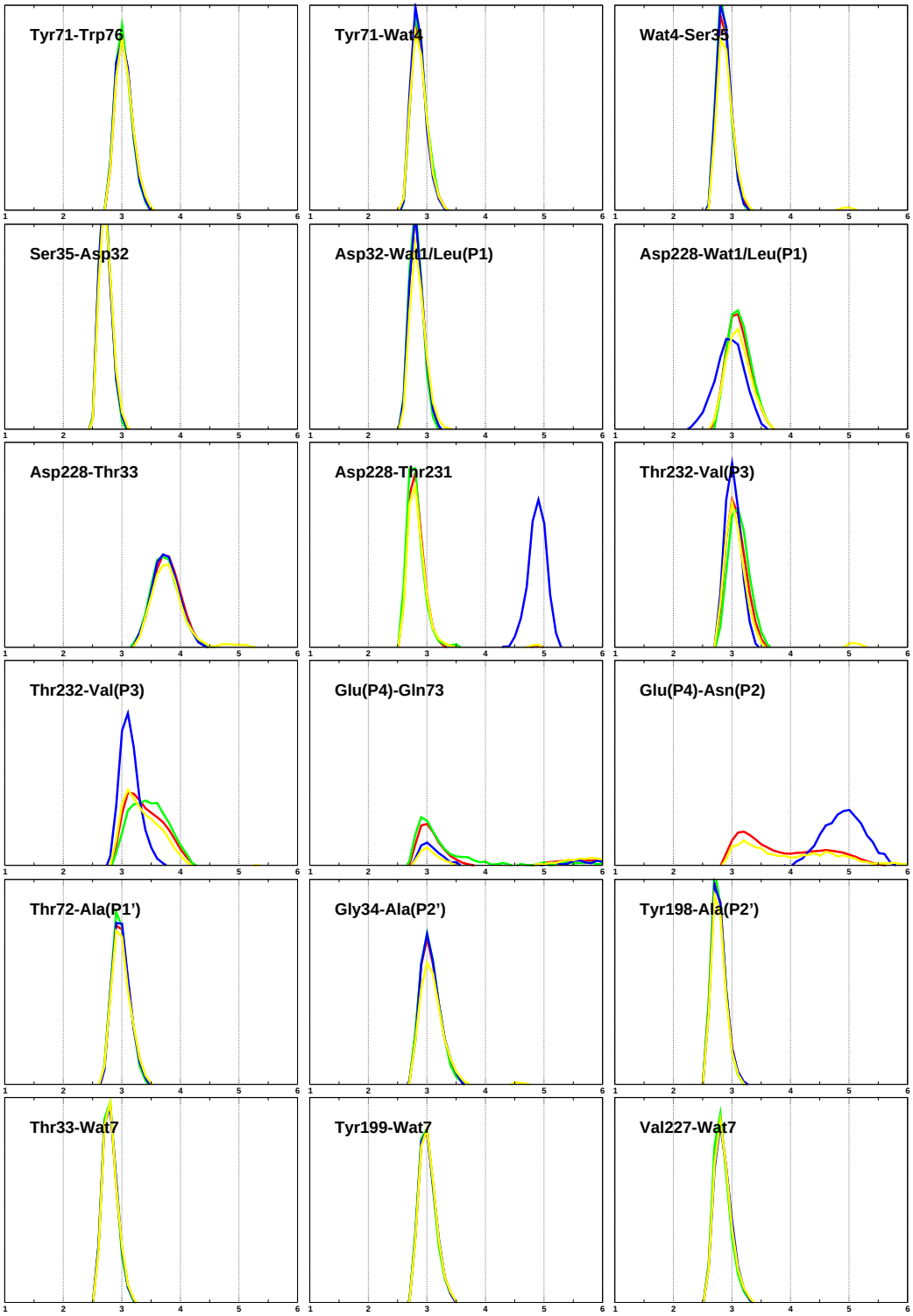

Figure S13: Same as in Figure S11 for BACE-intermediate state. The distribution in the cFEP basins A through D (Figure 6a of the main text) are shown in red, green, blue, and yellow, respectively.

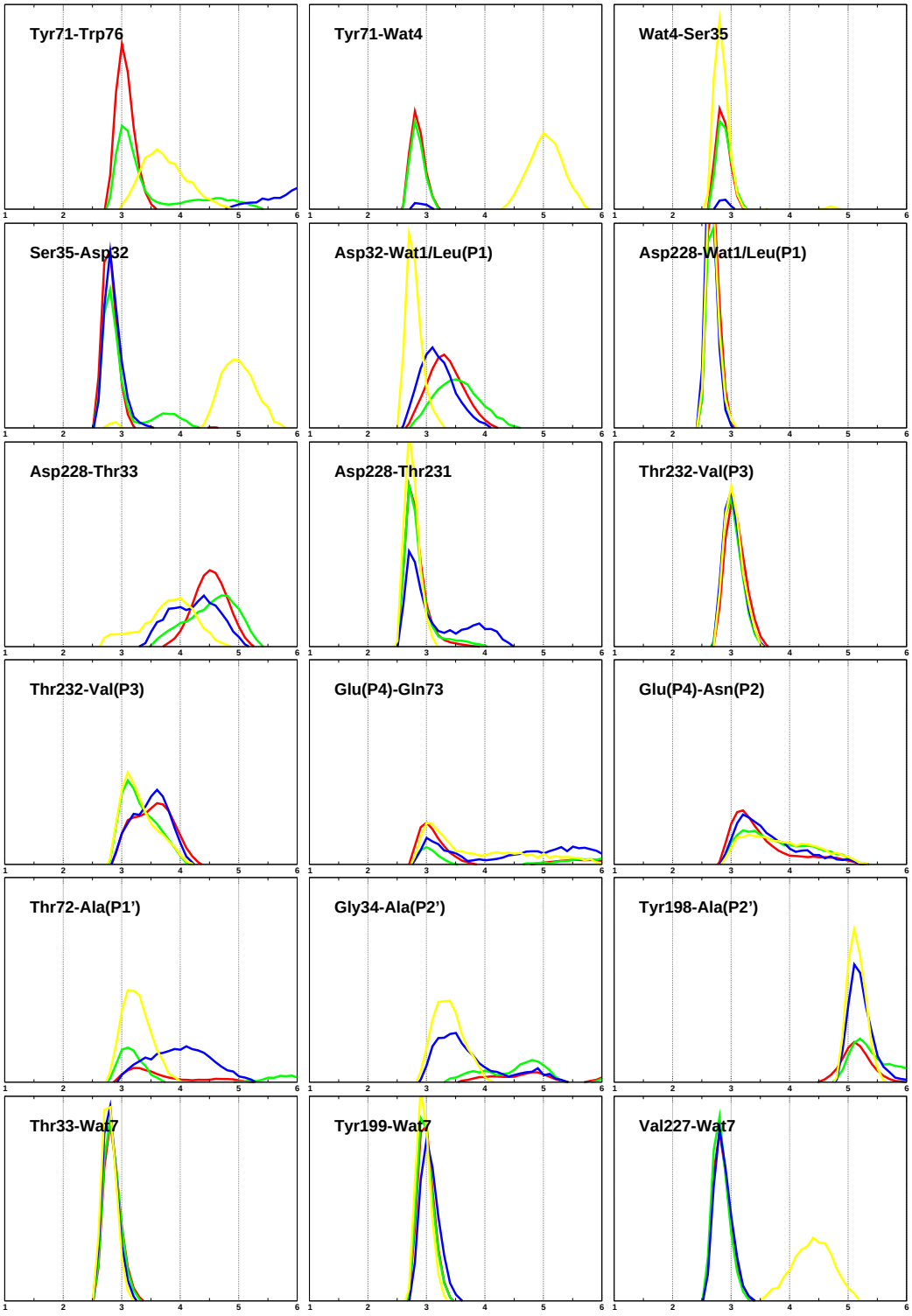

Figure S14: Same as in Figure S11 for BACE-product state. The distribution in the cFEP basins A through D (Figure 8a of the main text) are shown in red, green, blue, and yellow, respectively.

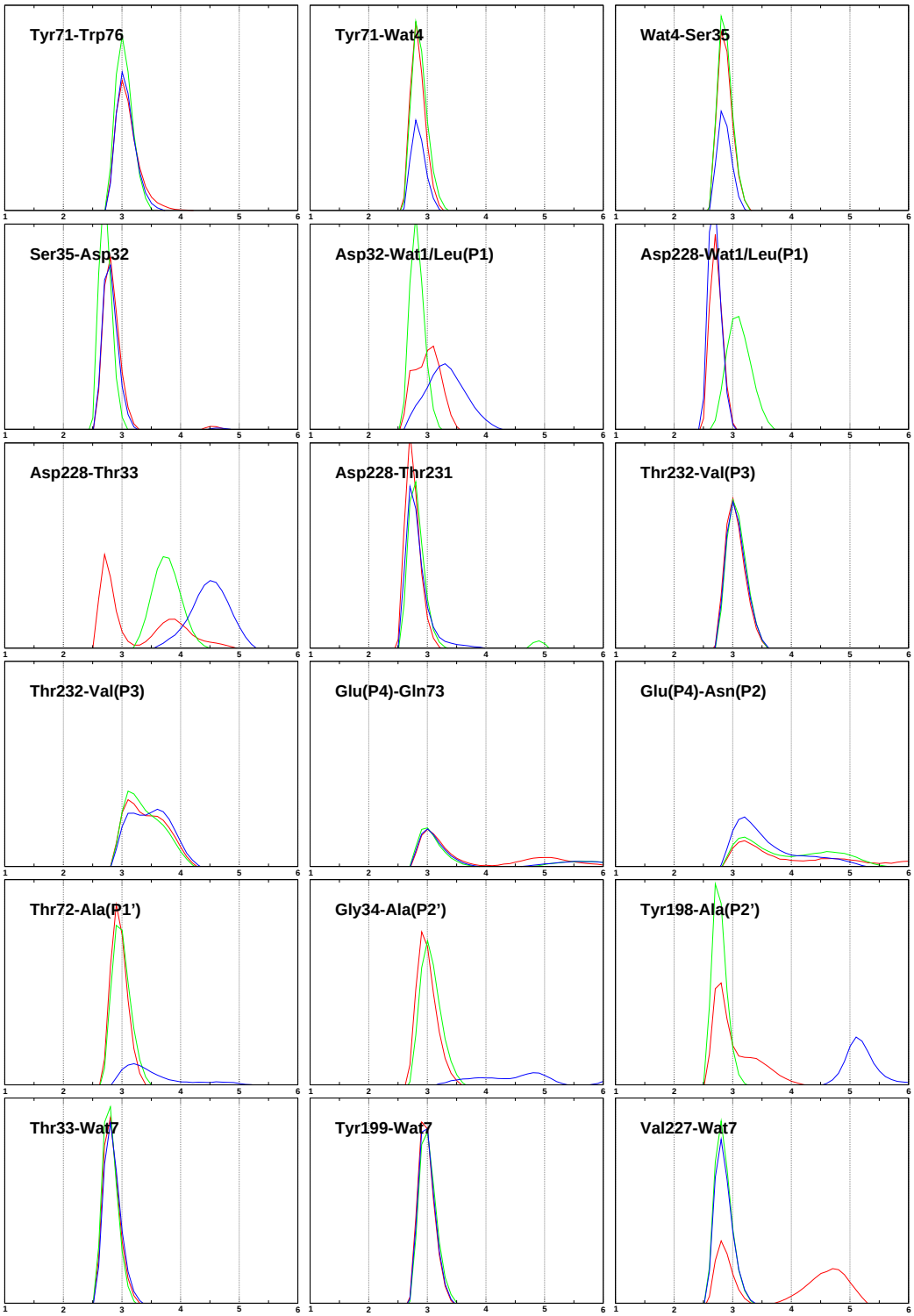

Figure S15: Distribution of the heavy-atom distances (in Å) of hydrogen bond partners in BACE active site and substrate, when substrate is in reactant (red), intermediate (green), and product (blue) state.

Complete citation for References 2, 41, and 44 of the main text:

2. Vassar, R., Bennett, B., Babu-Khan, S., Kahn, S., Mendiaz, E., Denis, P., Teplow, D., Ross, S., Amarante, P., Loeloff, R., Luo, Y., Fisher, S., Fuller, J., Edenson, S., Lile, J., Jarosinski, M., Biere, A., Curran, E., Burgess, T., Louis, J., Collins, F., Treanor, J., Rogers, G., Citron, M. (1999) β-secretase cleavage of Alzheimer's amyloid precursor protein by the transmembrane aspartic protease BACE. *Science 286*, 735–741

41. MacKerell, Jr., A. D., Bashford, D., Bellott, M., Dunbrack, Jr., R. L., Evan-seck, J. D., Field, M. J., Fischer, S. , Gao, J., Guo, H., Ha, S., Joseph-McCarthy, D., Kuchnir, L., Kuczera, K., Lau, F. T. K., Mattos, C., Michnick, S., Ngo, T., Nguyen, D. T., Prodhom, B., Reiher, III W. E., Roux, B., Schlenkrich, M., Smith, J. C., Stote, R., Straub, R., Watanabe, R., Wiorkiewicz-Kuczera, J., Yin, D., Karplus, M. J. (1998) All atom empirical potential for molecular modeling and dynamics studies of proteins. *J. Phys. Chem. B 102*, 3586–3616

44. Brooks, B. R., Brooks, C. L., Mackerell, A. D., Nilsson, L., Petrella, R. J., Roux, B., Won, Y., Archontis, G., Bartels, C., Boresch, S., Caflisch, A., Caves, L., Cui, Q., Dinner, A. R., Feig, M., Fischer, S., Gao, J., Hodoscek, M., Im, W., Kuczera, K., Lazaridis, T., Ma, J., Ovchinnikov, V., Paci, E., Pastor, R. W., Post, C. B., Pu, J. Z., Schaefer, M., Tidor, B., Venable, R. M., Woodcock, H. L., Wu, X., Yang, W., York, D. M., Karplus, M. (2009) CHARMM: the biomolecular simulation program. *J. Comput. Chem. 30*, 1545–1614